

# Raman spectroscopy and microwave dielectric properties of Sn substituted SrLa<sub>4</sub>Ti<sub>5</sub>O<sub>17</sub> ceramics

ABDUL MANAN<sup>1\*</sup>, ATTA ULLAH<sup>2</sup>, ARBAB SAFEER AHMAD<sup>1</sup>

<sup>1</sup>Department of Physics, University of Science and Technology Bannu, 28100, KPK, Pakistan

<sup>2</sup>School of Materials Science and Engineering, Wuhan University of Technology, Wuhan, 430070, China

<sup>3</sup>Department of Physics, Islamia College Peshawar, 25120 Peshawar, Pakistan

SrLa<sub>4</sub>Ti<sub>5-x</sub>Sn<sub>x</sub>O<sub>17</sub> ( $0 \leq x \leq 2$ ) ceramics were fabricated through solid state ceramic route and their microwave dielectric properties were investigated in an attempt to tune their temperature coefficient of resonant frequency ( $\tau_f$ ) to zero. The compositions were sintered to single phase SrLa<sub>4</sub>Ti<sub>5</sub>O<sub>17</sub> and SrLa<sub>4</sub>Ti<sub>4.5</sub>Sn<sub>0.5</sub>O<sub>17</sub> ceramics at  $x = 0$  and  $x = 0.5$ , and SrLa<sub>4</sub>Ti<sub>4-x</sub>Sn<sub>x</sub>O<sub>17</sub> along with a small amount of La<sub>2</sub>Ti<sub>2</sub>O<sub>7</sub> at  $x = 1$ . The major phase observed at  $x = 2$  was La<sub>2</sub>Ti<sub>2</sub>O<sub>7</sub> but along with SrLa<sub>4</sub>Ti<sub>4</sub>SnO<sub>17</sub> and SrLa<sub>4</sub>Ti<sub>4</sub>O<sub>15</sub> as the secondary phases.  $\tau_f$  decreased from 117 to 23.0 ppm/°C but at the cost of dielectric constant ( $\epsilon_r$ ) and quality factor multiplied by resonant frequency ( $Q_u f_o$ ) which decreased from 65 to 33.6 and 11150 to 4191 GHz, respectively. The optimum microwave dielectric properties, i.e.  $\tau_f = 38.6$  ppm/°C,  $\epsilon_r = 45.5$  and  $Q_u f_o = 7919$  GHz, correspond to the SrLa<sub>4</sub>Ti<sub>5-x</sub>Sn<sub>x</sub>O<sub>17</sub> composition with  $x = 1$ .

Keywords: *ceramics; microwave properties; Raman spectroscopy; SEM*

© Wrocław University of Technology.

## 1. Introduction

Lead free dielectric oxide ceramics with high electric permittivity ( $\epsilon_r$ ), high unloaded quality factor ( $Q_u$ ) and a near zero temperature coefficient of resonant frequency ( $\tau_f$ ) are critical elements in the components, such as resonators, oscillators and filters for wireless communication. For commercial applications, any material used as a dielectric resonator must have  $\epsilon_r > 24$ ,  $Q_u f_o > 30,000$  GHz and  $|\tau_f| \leq 3$  ppm/°C [1]. For certain applications, such as antennas, the requirements for low  $\tau_f$  and high  $Q_u f_o$  are flexible but  $\epsilon_r$  is generally required to be as high as possible to miniaturize the device so that it might be incorporated into a handset [2]. Recently, layered perovskites with a general formula  $A_n B_n O_{3n+2}$  (where A and B are cations) have received much attention due to their high dielectric performance and applications in patch antennas. Jawahar et al. [2] reported CaLa<sub>4</sub>Ti<sub>5</sub>O<sub>17</sub> with  $\epsilon_r = 53$ ,

$\tau_f = -20$  ppm/°C and  $Q_u f_o = 17359$  GHz that was sintered at 1625 °C. The microwave dielectric properties of CaLa<sub>4</sub>Ti<sub>5</sub>O<sub>17</sub> ceramics were improved by substituting Ca<sup>2+</sup> ions with Zn<sup>2+</sup> ions [4].  $\epsilon_r = 57$ ,  $Q_u f_o = 15,000$  GHz, and  $\tau_f = -8.16$  ppm/°C were obtained for Ca<sub>0.99</sub>Zn<sub>0.01</sub>La<sub>4</sub>Ti<sub>5</sub>O<sub>17</sub> ceramics with 0.5 wt.% CuO additive that were sintered at 1450 °C for 4 h [5]. On the other hand, SrLa<sub>4</sub>Ti<sub>5</sub>O<sub>17</sub> was reported to have  $\epsilon_r = 61$ ,  $Q_u f_o = 9969$  GHz and  $\tau_f = 117$  ppm/°C [3]. The high positive  $\tau_f$  precluded its use as dielectrically loaded antenna. In previous studies, Sm and Nd substitution for La in SrLa<sub>4</sub>Ti<sub>5</sub>O<sub>17</sub> resulted in  $\tau_f \sim 0$  ppm/°C but at a cost of a decrease in  $Q_u f_o$  to 3000 GHz and 6000 GHz, respectively [6, 7]. The substitution of Sn<sup>4+</sup> for Ti<sup>4+</sup> has been reported to lower  $\tau_f$  of some compounds, for example, Ba<sub>4</sub>LaMnNb<sub>3</sub>O<sub>15</sub> (M = Ti, Sn) [8, 9] without any significant effect on the  $Q_u f_o$ ; therefore, in the present study, the effects of Sn<sup>4+</sup> substitution for Ti<sup>4+</sup> on the phase, microstructure and microwave dielectric properties of SrLa<sub>4</sub>Ti<sub>5-x</sub>Sn<sub>x</sub>O<sub>17</sub> ( $0 \leq x \leq 2$ ) ceramics were

\*E-mail: drmanan82@yahoo.com

investigated in an attempt to lower  $\tau_f$  of the resulting compounds.

## 2. Experimental

$\text{SrLa}_4\text{Ti}_{5-x}\text{Sn}_x\text{O}_{17}$  ( $0 \leq x \leq 2$ ) batch compositions were prepared by weighing the required amounts of  $\text{SrCO}_3$  (Aldrich, 99+ %),  $\text{La}_2\text{O}_3$  (Aldrich, 99.95 %),  $\text{TiO}_2$  (Aldrich, anatase, 99+ %) and  $\text{SnO}_2$  (Aldrich, 99.95 %). The mixed batches were ball milled for 24 h in polyethylene disposable mill-jars using Y-toughened  $\text{ZrO}_2$  balls as grinding media and isopropanol as lubricant to make freely flowing slurries. The resulting slurries were dried in and oven kept at 95 °C for about 24 h and then calcined at 1250 °C to 1300 °C for 6 h at a heating/cooling rate of 5 °C/min. The calcined powders were finely ground in an agate pestle and mortar for 45 min and then pressed into 4 to 5 mm high and 10 mm diameter pellets in a steel die at 80 MPa. The pellets were sintered at 1450 to 1650 °C for 4 h at a heating/cooling rate of 5 °C/min. Densities of the sintered pellets were measured using Archimedes method. Phase analysis of the sintered samples was carried out using a Philips X-ray diffractometer (XRD) with  $\text{CuK}\alpha$  radiation ( $\lambda = 1.5406 \text{ \AA}$ ) operating at 30 kV and 40 mA at  $1^\circ/\text{min}$  in  $2\theta = 10$  to  $70^\circ$  with a step size of  $0.02^\circ$ . A Renishaw's inVia Raman microscope was used for Raman measurements. The microwave dielectric properties were measured using a R3767CH Agilent network analyzer by placing the cylindrical pellets on a low loss quartz single crystal at the center of an Au-coated brass cavity.  $\tau_f$  was measured by measuring the temperature variation of  $\text{TE}_{018}$  resonance mode in the temperature range of 20 to 80 °C.

## 3. Results and discussion

Fig. 1 shows the XRD patterns recorded at room temperature for optimally sintered  $\text{SrLa}_4\text{Ti}_{5-x}\text{Sn}_x\text{O}_{17}$  ( $0 \leq x \leq 2$ ) ceramics. The patterns of the compositions with  $x = 0, 0.5$  and 1 were identical and matched with the one reported for  $\text{SrLa}_4\text{Ti}_5\text{O}_{17}$  (PDF# 57-00940) but with an appropriate shift in the peaks positions towards

lower angles for the samples with  $x = 0.5$  and 1 due to the presence of relatively larger Sn ions at the B-site of the perovskite unit cell. This indicated the formation of some  $\text{SrLa}_4\text{Ti}_{4.5}\text{Sn}_{0.5}\text{O}_{17}$  and  $\text{SrLa}_4\text{Ti}_4\text{SnO}_{17}$  compounds containing isostructural phases with  $\text{SrLa}_4\text{Ti}_5\text{O}_{17}$  at  $x = 0.5$  and 1. The presence of a few low intensity XRD peaks indicated the beginning of the formation of a secondary  $\text{La}_2\text{Ti}_2\text{O}_7$  (PDF# 70-1690) phase at  $x = 1$ . At  $x = 2$ ,  $\text{La}_2\text{Ti}_2\text{O}_7$  (PDF# 70-1690) was observed as the major phase but along with  $\text{SrLa}_4\text{Ti}_4\text{SnO}_{17}$  and  $\text{SrLa}_4\text{Ti}_4\text{O}_{15}$  (PDF# 49-0254) as minor phases. The observed increase in the intensity of the XRD peaks due to  $\text{La}_2\text{Ti}_2\text{O}_7$  indicated an increase in their amount with increasing  $x$ .

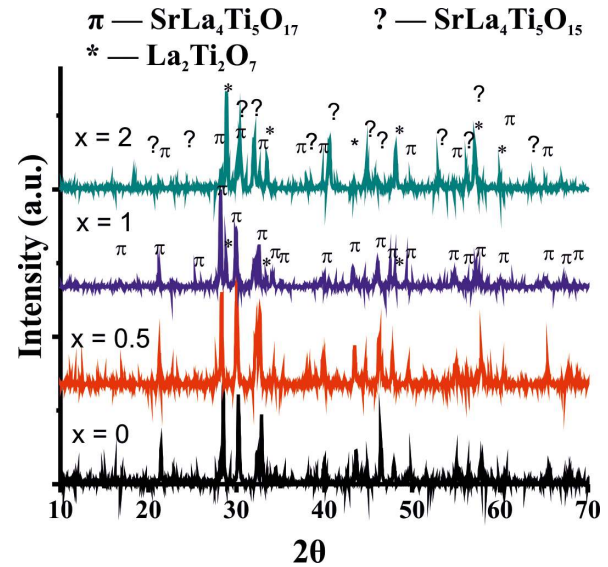


Fig. 1. XRD patterns of  $\text{SrLa}_4\text{Ti}_{5-x}\text{Sn}_x\text{O}_{17}$  ( $0 \leq x \leq 2$ ) ceramics, showing the formation of  $\text{SrLa}_4\text{Ti}_5\text{O}_{17}$ ,  $\text{SrLa}_4\text{Ti}_{4.5}\text{Sn}_{0.5}\text{O}_{17}$  at  $x = 0$  and 0.5,  $\text{SrLa}_4\text{Ti}_4\text{SnO}_{17}$  along with  $\text{La}_2\text{Ti}_2\text{O}_7$  at  $x = 1$  and  $\text{La}_2\text{Ti}_2\text{O}_7$  and  $\text{SrLa}_4\text{Ti}_4\text{O}_{15}$  along with a few diminishing peaks due to  $\text{SrLa}_4\text{Ti}_4\text{SnO}_{17}$  at  $x = 2$ .

The secondary electron images (SEIs) of thermally etched and gold-coated surfaces of  $\text{SrLa}_4\text{Ti}_{5-x}\text{Sn}_x\text{O}_{17}$  ( $0 \leq x \leq 2$ ) ceramics sintered at their optimum sintering temperatures are shown in Fig. 2. The microstructure of the compositions with  $x = 0$ , and 0.5 comprised of elongated grains of the size ranging from  $1 \times 1 \mu\text{m}^2$  to  $5 \times 7 \mu\text{m}^2$  and  $1 \times 3 \mu\text{m}^2$  to  $5 \times 20 \mu\text{m}^2$  (Fig. 2a

and Fig. 2b). Semi-quantitative SEM EDS (Table 1) of the grains labeled as “A” and “B” indicated that the composition of these grains was close to SrLa<sub>4</sub>Ti<sub>5</sub>O<sub>17</sub> and SrLa<sub>4</sub>Ti<sub>4.5</sub>Sn<sub>0.5</sub>O<sub>17</sub>, respectively. Generally, the microstructure of the composition with  $x = 1$  also comprised of elongated rod and plate-shaped grains labeled as “c” (Fig. 2c), where the molar elemental composition of these grains was close to SrLa<sub>4</sub>Ti<sub>4</sub>SnO<sub>17</sub> (Table 1). The microstructure of the composition with  $x = 2$  comprised of micro-regions including cubical grains labeled as “D” (Fig. 2d). Semi-quantitative EDS (Table 1) indicated that the composition of these grains was close to La<sub>2</sub>Ti<sub>2</sub>O<sub>7</sub> phase as the EDS detected little Sr or Sn in these grains. This suggested the presence of grains due to La<sub>2</sub>Ti<sub>2</sub>O<sub>7</sub> phase as observed by XRD of the same composition. The observed variation in the composition of the grains (Table 1) combined with the morphological change from rod-shaped grains to cubical grains with an increase in Sn content indicated the formation of secondary phases.

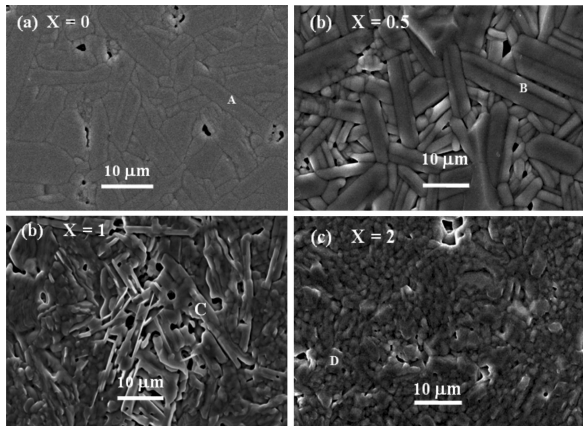


Fig. 2. SEIs recorded from thermally etched, gold-coated sintered SrLa<sub>4</sub>Ti<sub>5-x</sub>Sn<sub>x</sub>O<sub>17</sub> compositions showing (a) elongated grains at  $x = 0$ , (b) elongated grains at  $x = 0.5$ , (c) elongated grains at  $x = 1$ , (d) cuboidal shaped grains at  $x = 2$ .

The change from one compound to another with compositions can also be proved by Raman spectra analysis.

Raman spectroscopy is considered to be an ideal tool for probing the degree of cation ordering, also suitable to study dynamic changes in

a structure. Fig. 3 illustrates the Raman spectra of SrLa<sub>4</sub>Ti<sub>5-x</sub>Sn<sub>x</sub>O<sub>17</sub> ( $0 \leq x \leq 2$ ) ceramics. The spectra are very similar to those of the related compounds in the Ca<sub>1-x</sub>Zn<sub>x</sub>La<sub>4</sub>Ti<sub>5</sub>O<sub>17</sub> series [4]. Generally, corner shared and edge-shared octahedra are predominant in (Nb, Ti)-O polyhedra. In the corner-shared octahedra, the symmetric stretching vibrations are observed in the 750 to 850 cm<sup>-1</sup> region [10].

Table 1. Elemental composition (in moles) calculated from semi-quantitative EDS data of the grains labelled in Fig. 2.

Grain	Sr	La	Ti	Sn
A	1	4.12	4.26	0
B	1	4.10	4.20	0.6
C	2.95	10.17	9.36	1
D	1.35	13.93	15.09	1

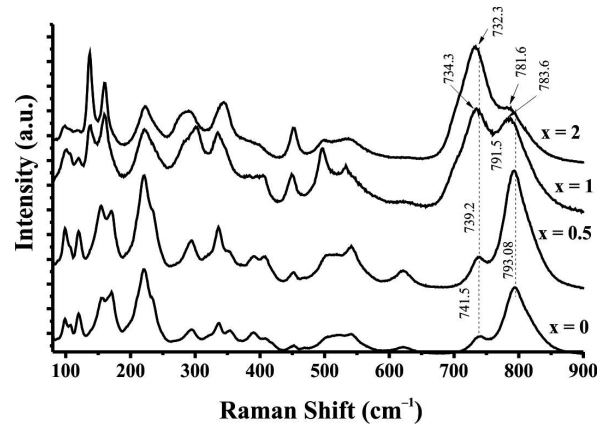


Fig. 3. Raman spectra recorded at room temperature for SrLa<sub>4</sub>Ti<sub>5-x</sub>Sn<sub>x</sub>O<sub>17</sub> ( $0 \leq x \leq 2$ ) compositions.

In the present study, the highest frequency A<sub>1g</sub> mode at 793.08 cm<sup>-1</sup> for  $x = 0$  corresponds to the symmetric metal-oxygen stretching vibrations of the BO<sub>6</sub> octahedra, but it is shifted towards lower frequency of 781 cm<sup>-1</sup> as the value of  $x$  increased from 0 to 2, along with a decrease in its intensity. This is due to the incorporation of bigger cation of Sn<sup>4+</sup> (0.69 Å) in place of smaller cation of Ti<sup>4+</sup> (0.605 Å) [11] which induced a decrease in the force constant or the stiffness of the oxygen octahedral cage as a result of the covalent

character of the central  $\text{TiO}_6$  octahedra [4]. The vibrational modes in the  $750$  to  $850\text{ cm}^{-1}$  region, supported the existence of the corner shared octahedra in the  $\text{SrLa}_4\text{Ti}_{5-x}\text{Sn}_x\text{O}_{17}$  series of compounds. The XRD revealed  $\text{La}_2\text{Ti}_2\text{O}_7$  as the major phase and  $\text{SrLa}_4\text{Ti}_4\text{O}_{15}$  as the secondary phase with the increase in peak intensities. Since  $\text{La}_2\text{Ti}_2\text{O}_7$  has only one cation at the B site, no  $A_{1g}$  Raman mode was active. The new Raman active mode band with increased intensity that appeared at  $734\text{ cm}^{-1}$ , suppressing the  $A_{1g}$  mode at  $781\text{ cm}^{-1}$  for  $x \geq 1$ , could be attributed to the  $A_{1g}$  mode of  $\text{BO}_6$  octahedra in  $\text{SrLa}_4\text{Ti}_4\text{O}_{15}$  ceramics that developed as a secondary phase along with  $\text{La}_2\text{Ti}_2\text{O}_7$  as a major phase. The weak band observed at  $605$  to  $620\text{ cm}^{-1}$  range can be assigned to the B–O symmetric stretching vibration [12, 13]. The broad bands at  $450$  to  $570\text{ cm}^{-1}$  can be represented as symmetric breathing of the  $\text{BO}_6$  octahedra [14]. The  $E_g$  modes in the range of  $200$  to  $400\text{ cm}^{-1}$  have been assigned to O–B–O bending mode [12]. The modes in the range of  $470$  to  $490\text{ cm}^{-1}$  were described as B–O torsional modes [15]. The modes at  $314$  and  $464\text{ cm}^{-1}$  can be attributed to the rotating and tilting of the  $\text{BO}_6$  octahedron [15]. The intensity of the bands around  $250$  to  $350\text{ cm}^{-1}$  increased with an increase in the  $x$  value and also shifted towards higher frequencies.

The modes below  $250\text{ cm}^{-1}$  can be assigned to lattice vibrations of the A-site cations.

The microwave dielectric properties of  $\text{SrLa}_4\text{Ti}_{5-x}\text{Sn}_x\text{O}_{17}$  ( $0 \leq x \leq 2$ ) ceramics sintered at their optimum sintering temperatures are shown in Fig. 4 and Fig. 5 and are also compared in Table 2.  $\epsilon_r$ ,  $\tau_f$  and  $Q_u f_0$  were observed to decrease from  $65.0$  to  $33.8$ ,  $118\text{ ppm}/^\circ\text{C}$  to  $21.0\text{ ppm}/^\circ\text{C}$  and  $11150\text{ GHz}$  to  $4191\text{ GHz}$  with an increase in  $\text{Sn}^{4+}$  content from  $0$  to  $2$ , respectively. It has been reported that the substitution of  $\text{Sn}^{4+}$  for  $\text{Ti}^{4+}$  caused a decrease in  $\epsilon_r$ , hence,  $\tau_f$  in other compounds [9]. Therefore, the observed decrease in  $\epsilon_r$  (Fig. 4) could be attributed to the less ionic dielectric polarizability ( $2.83\text{ \AA}^3$ ) of  $\text{Sn}^{4+}$  in comparison to ( $2.93\text{ \AA}^3$ ) of  $\text{Ti}^{4+}$  [16]. However, for  $1 \leq x \leq 2$ , the decrease in  $\epsilon_r$  could be attributed to

the formation of the secondary phase of  $\text{La}_2\text{Ti}_2\text{O}_7$  with  $\epsilon_r = 22$  [4]. The observed decrease in  $Q_u f_0$  (Fig. 5) upon increasing Sn content from  $1$  to  $2$  may be due to the formation of secondary phases, whose interface causes additional dielectric loss [10].  $\tau_f$  decreased from  $117$  to  $23.0\text{ ppm}/^\circ\text{C}$  (Fig. 4) with the increase in  $x$  from  $0$  to  $2$  but at the cost of  $\epsilon_r$  and  $Q_u f_0$  which decreased from  $65$  to  $33.6$  and  $11150$  to  $4339\text{ GHz}$ , respectively, due to the formation of secondary phases which made higher concentrations of Sn unfavorable. Thus, the optimum microwave dielectric properties ( $\tau_f = 39\text{ ppm}/^\circ\text{C}$ ,  $\epsilon_r = 46$  and  $Q_u f_0 = 7900\text{ GHz}$ ), corresponded to the  $\text{SrLa}_4\text{Ti}_{5-x}\text{Sn}_x\text{O}_{17}$  composition with  $x = 1$  with minimum Sn content, hence, the secondary phases.

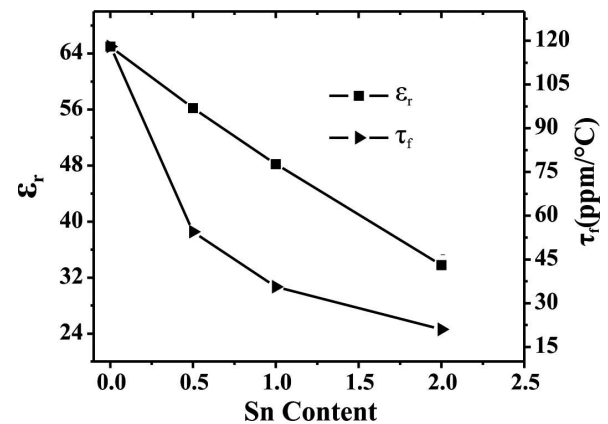


Fig. 4. Variation in  $\epsilon_r$  and  $\tau_f$  versus  $\text{Sn}^{4+}$  content ( $x$ ) for  $\text{SrLa}_4\text{Ti}_{5-x}\text{Sn}_x\text{O}_{17}$  ( $0 \leq x \leq 2$ ) compositions sintered at their optimum sintering temperatures.

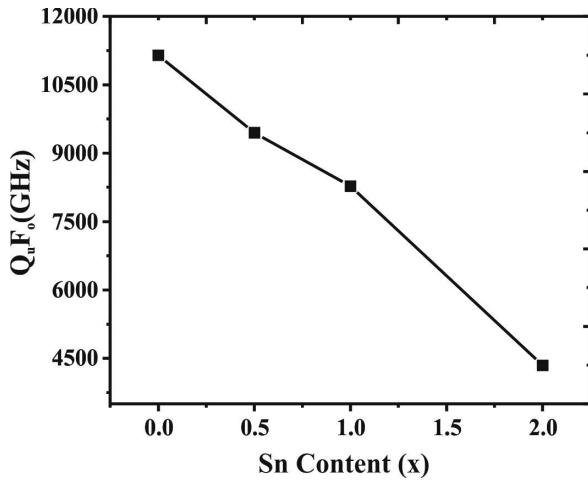
## 4. Conclusions

$\text{SrLa}_4\text{Ti}_{5-x}\text{Sn}_x\text{O}_{17}$  compositions crystallize into single phase ceramics at  $x = 0$ , and  $x = 0.5$ , while the formation of a small amount of second phase begins at  $x = 1$ . The substitution of Sn for Ti causes a substantial decrease in  $\tau_f$  but at a cost of  $\epsilon_r$  and  $Q_u f_0$  due to the second phase formation, which makes higher concentration of Sn unfavorable. The optimum microwave dielectric properties, i.e.  $\tau_f = 35.6\text{ ppm}/^\circ\text{C}$ ,

Table 2. Preparation conditions, apparent densities and microwave dielectric properties of SrLa<sub>4</sub>Ti<sub>5-x</sub>Sn<sub>x</sub>O<sub>17</sub> (0 ≤ x ≤ 2).

x	CT [°C]	ST [°C]	ρ <sub>exp</sub> [g/cm <sup>3</sup> ]	ε <sub>r</sub>	Q <sub>u</sub> f <sub>o</sub> [GHz]	τ <sub>f</sub> [ppm/°C]
0	1250/6h	1500/4h	5.41	65.0	11150	+118
0.5	1300/6h	1600/4h	5.63	56.2	9450	+54.5
1	1300/6h	1625/4h	5.60	48.2	8278	+35.6
2	1300/6h	1625/4h	5.75	33.8	4345	+21.0

CT = Calcination temperature, ST = Sintering temperature, ρ<sub>ap</sub> = Apparent density

Fig. 5. Variation in Q<sub>u</sub>f<sub>o</sub> versus Sn<sup>4+</sup> content (x) for SrLa<sub>4</sub>Ti<sub>5-x</sub>Sn<sub>x</sub>O<sub>17</sub> (0 ≤ x ≤ 2) compositions sintered at their optimum sintering temperatures.

ε<sub>r</sub> = 48.6 and Q<sub>u</sub>f<sub>o</sub> = 8278 GHz, correspond to the SrLa<sub>4</sub>Ti<sub>5-x</sub>Sn<sub>x</sub>O<sub>17</sub> composition with x = 1.

### Acknowledgements

The authors acknowledge the financial support of the Higher Education Commission of Pakistan under the International Research Support Initiative Program (IRSIP) Scheme and the Electroceramics group at the department of Materials Science and Engineering University of Sheffield UK.

### References

- [1] REANEY I.M., IDLES D., *J. Am. Ceram. Soc.*, 89 (2006), 2068
- [2] JAWAHAR I.N., SANTHA N.I., SEBASTIAN M.T., MOHANAN P., *J. Mater. Res.*, 17 (2002), 3084.
- [3] IQBAL Y., MANAN A., REANEY I.M., *Mater. Res. Bull.*, 46 (2011), 1092.
- [4] FEI Z.Y., *J. Am. Ceram. Soc.*, 89 (2006), 3421.
- [5] CHEN Y.C., TSAI J.M., *Jpn. J. Appl. Phys.*, 47 (2008), 7959.
- [6] MANAN A., IQBAL Y., *J. Mater. Sci. Mater. Electron.*, 22 (2011), 1848.
- [7] MANAN A., IQBAL Y., *Mater. Res. Bull.*, 47 (2012), 883.
- [8] FANG L., *Mater. Res. Bull.*, 39 (2004), 1649.
- [9] MANAN A., HUSSAIN I., *Int. J. Mod. Phys. B*, 28 (2014), 1450092.
- [10] RATHEESH R., SREEMOOLANADHAN H., SEBASTIAN M.T., *J. Solid State. Chem.*, 131 (1997), 2.
- [11] SHANNON R.D., *Acta. Crystallogr. A*, 32 (751) (1976), 751.
- [12] ZHENG H., *J. Mater. Res.*, 19 (2004), 488.
- [13] LEVIN I., *J. Solid State. Chem.*, 156 (2001), 122.
- [14] HIRATA T., ISHIOKA K., KITAJIMA M., *J. Solid State. Chem.*, 124 (1996), 353.
- [15] HAO H., *Appl. Phys. A*, 85 (2006), 69.
- [16] SHANNON R.D., *J. Appl. Phys.*, 73 (1993), 348.

Received 2014-08-24

Accepted 2015-11-11